Mcp5, a meiotic cell cortex protein, is required for nuclear movement mediated by dynein and microtubules in fission yeast

Takamune T. Saito, Daisuke Okuzaki, and Hiroshi Nojima

Department of Molecular Genetics, Research Institute for Microbial Diseases, Osaka University, Suita, Osaka 565-0871, Japan

THE JOURNAL OF CELL BIOLOGY

During meiotic prophase I of the fission yeast *Schizosaccharomyces pombe*, oscillatory nuclear movement occurs. This promotes homologous chromosome pairing and recombination and involves cortical dynein, which plays a pivotal role by generating a pulling force with the help of an unknown dynein anchor. We show that Mcp5, the homologue of the budding yeast dynein anchor Num1, may be this putative dynein anchor. *mcp5*⁺ is predominantly expressed during meiotic prophase, and GFP-Mcp5 localizes at the cell cortex. Moreover, the *mcp5Δ* strain lacks the oscillatory nuclear movement. Accordingly, homologous pairing and recombination rates of the *mcp5Δ* strain are significantly reduced. Furthermore, the cortical localization of dynein heavy chain 1 appears to be reduced in *mcp5Δ* cells. Finally, the full function of Mcp5 requires its coiled-coil and pleckstrin homology (PH) domains. Our results suggest that Mcp5 localizes at the cell cortex through its PH domain and functions as a dynein anchor, thereby facilitating nuclear oscillation.

Introduction

The formation of heritable haploid gametes from diploid parental cells requires meiosis, a special type of cell division. After premeiotic DNA replication, homologous chromosome pairing and genetic recombination occur during prophase I with formation of bouquet arrangement conserved among species (for review see Harper et al., 2004). During prophase I of fission yeast, horsetail nuclear movement occurs. It starts when all the telomeres become bundled at the spindle pole body (SPB; Hiraoka, 1998). Subsequently, the nucleus undergoes a dynamic oscillation, resulting in elongated nuclear morphology (Chikashige et al., 1994). This event has been proposed to facilitate the pairing of homologous chromosomes because it aligns the chromosomes in the same direction (through the bundling of their telomeric ends) and then shuffles them around each other (Chikashige et al., 1994; Kohli, 1994; Niwa et al., 2000; Ding et al., 2004).

It has been proposed that horsetail nuclear movement is predominantly due to the pulling of astral microtubules that link the SPB to cortical microtubule-attachment sites at the opposite end of the cell; the pulling force is believed to be provided by cytoplasmic dynein (Ding et al., 1998; Yamamoto et al., 1999; Yamamoto and Hiraoka, 2003) and the dynactin (Yamashita

et al., 1997; Niccoli et al., 2004) complex. However, the details of these mechanisms are still almost completely unknown. A key to understanding nuclear oscillation is the identification and characterization of the anchor protein at the cell cortex that binds to dynein. We report that a novel meiosis-specific gene named *mcp5*⁺ (from meiotic coiled-coil protein) encodes a protein, Mcp5 (Saito et al., 2005), that functions as this anchor during the meiosis of *Schizosaccharomyces pombe*. Recently, we found that it is also registered as Mug21 (Martin-Castellanos et al., 2005). Mcp5/Mug21 is homologous to Num1 (nuclear migration) of *Saccharomyces cerevisiae*, ApsA (anucleate primary sterigmata) of *Aspergillus nidurans*, and Ami1 (anucleate microconidia) of *Podospra anserina*, but these Num1-like proteins function during vegetative growth rather than in meiosis (Kormanec et al., 1991; Fischer and Timberlake, 1995; Graïa et al., 2000; Heil-Chapdelaine et al., 2000), unlike Mcp5. We demonstrate a contribution for such an anchoring mechanism in the process of homologue pairing during meiosis and establish a link between meiotic and mitotic nuclear behavior, albeit in different organisms.

Results and discussion

Oscillatory nuclear movement is absent in *mcp5Δ* cells

We first found that Mcp5 shows meiosis-specific expression and is essential for sporulation as shown in Fig. S1 (available

at http://www.jcb.org/cgi/content/full/jcb.200512129/DC1). Because *S. cerevisiae* Num1 is involved in nuclear migration during the budding process, we investigated the function of Mcp5 during the horsetail nuclear movement of *S. pombe*, which is the nuclear migration event in this species and which is specifically observed in meiotic prophase. We subjected h^{90} cells expressing DNA polymerase α-GFP to time-lapse observation under a microscope. In wild-type (WT) cells, sequential oscillatory nuclear movement is observed from karyogamy to slightly before meiosis I (Fig. 1 A and Video 1). In contrast, such oscillatory nuclear movement was not observed throughout prophase I in *mcp5Δ* cells (Fig. 1 B and Video 2). This abnormal oscillation was also observed in the azygotic meiosis of *mcp5Δ* cells (Videos 3 and 4). These data suggest that Mcp5 plays a significant role in nuclear oscillation.

In *mcp5Δ* cells, which show impaired horsetail movement (Fig. 1), the rates of pairing (Fig. S2, A and B; and Videos 5–8; available at http://www.jcb.org/cgi/content/full/jcb.200512129/DC1) and recombination (Fig. S2, C and D) of homologous chromo-

somes are also reduced. This is similar to what has been observed for the *mcp6/hrs1Δ* (Saito et al., 2005; Tanaka et al., 2005), *kms1Δ* (Shimanuki et al., 1997), *dhc1* mutant (Yamamoto et al., 1999), *dlc1Δ* (Miki et al., 2002), and *ssm4Δ* (Niccoli et al., 2004) cells, in which horsetail movement is also inhibited. Ectopic recombination rates are also increased in *mcp5Δ* cells (Fig. S2 E), as has also been observed for the *mcp6/hrs1Δ* (Saito et al., 2005) and *kms1Δ* (Niwa et al., 2000) cells.

We also found that the period from karyogamy to meiosis I in zygotic meiosis was 1.5 times longer in *mcp5Δ* cells than in WT cells (Fig. 1 C) and that the timing with which cells containing two or four nuclei peaked was similar in azygotic meiosis in both strains of *pat1* background (Fig. S2 F). These results suggest that the delay of prophase I in the zygotic meiosis of *mcp5Δ* cells is due to a delay in the progression of karyogamy. Both phenotypes of deficiency in nuclear movement and delay in karyogamy of *mcp5Δ* are similar to those of the *dhc1* mutant (Yamamoto et al., 1999).

Mcp5 localizes at the cell cortex during the horsetail phase

We examined the subcellular localization of Mcp5 by constructing a GFP-Mcp5–expressing strain in the h^{90} genetic background. Because the frequency of recombination of the *gfp-mcp5* cells was at the WT level (unpublished data), we judged the function of GFP-Mcp5 to be intact in this strain. The cells were induced to enter zygotic meiosis, observed by living and methanol fixation, and stained with Hoechst 33342 to detect the nucleus and with anti–α-tubulin antibody to detect the microtubules. As shown in Fig. 2 A (top), no GFP signal was detected during the vegetative phase. During the horsetail phase, however, the GFP-Mcp5 signals appeared in the cytoplasm with a gradient pattern, namely, seeping from the arm to the middle and from the arm to the cell end. Furthermore, some bright dots were detected at the cell cortex. Significantly, astral microtubules were observed to be elongating in the direction of some GFP-Mcp5 dots (Fig. 2 B). Notably, dynein heavy chain (Dhc) 1, one of the +TIPs (microtubule plus-end tracking proteins), colocalized with Mcp5 at a point of cell cortex during horsetail phase (Fig. 2 C). These cortical dots disappeared after the horsetail phase, and the signal was not detected again through meiosis I and II (Fig. 2 A). When Mcp5-GFP was overproduced in vegetative cells, Mcp5-GFP localized at the cell cortex, suggesting that other meiosis-specific proteins are not required for the cell cortex localization of Mcp5 (Fig. 2 D).

The cortical sliding of microtubules is abnormal in *mcp5Δ* cells

To examine the effect of Mcp5 on the sliding of microtubules at the cell cortex during the horsetail phase, h^{90} WT (YY105) and $h^{90}mcp5Δ$ (ST218-1) cells were chemically fixed 6 h after meiosis was induced by nitrogen starvation and then immunostained with anti-Sad1 antibody, and the tubulin-GFP image was observed under a microscope (Fig. 3, A and B). We counted only the cells at horsetail phase, at which point the microtubules exhibit a filamentous structure that extends from the SPB to the edge of the cell. We denoted the microtubules as "sliding" or
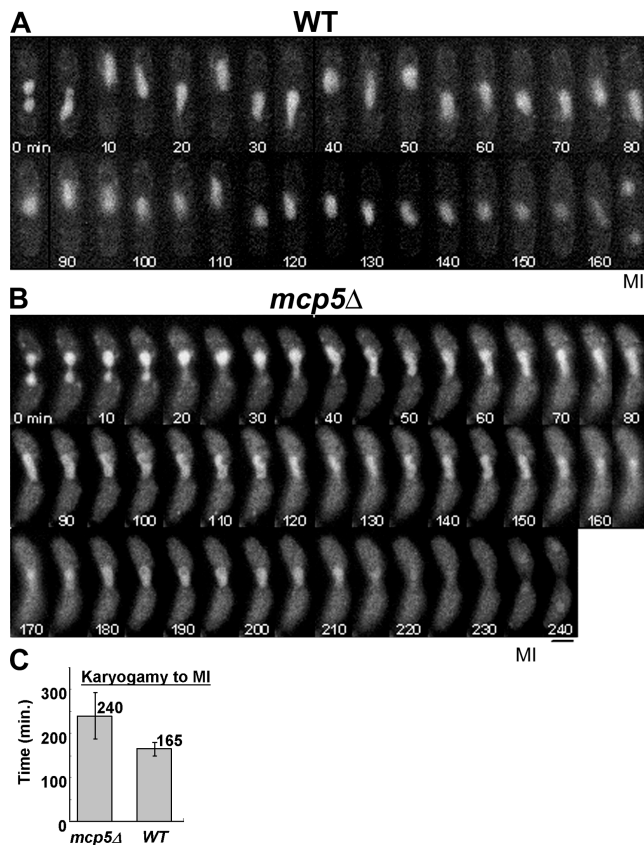

Figure 1. **Oscillatory nuclear movement is hampered at the horsetail phase in *mcp5Δ* cells.** (A and B) Time-lapse observation of WT (CT026-1; A) and *mcp5Δ* (ST205; B) cells during prophase I of zygotic meiosis. The nuclei were visualized by the fluorescence of the DNA polymerase α-GFP fusion construct. Single-cell images were obtained at 5-min intervals. The numbers at the bottom of each photograph represent the time in minutes, with 0 min being when nuclear fusion (karyogamy) starts. Bar, 5 μm. See Videos 1 and 2, available at http://www.jcb.org/cgi/content/full/jcb.200512129/DC1. (C) The duration of meiotic prophase, from the start of karyogamy to meiosis I chromosome segregation in WT and *mcp5Δ* cells. The mean values were calculated from 20 independent cells observed under a microscope. Standard deviations are shown as error bars.
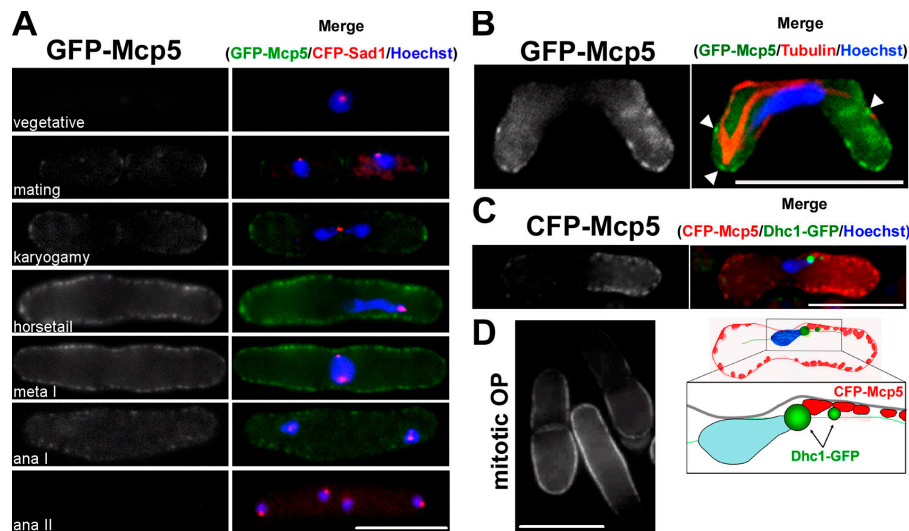
Figure 2. **Mcp5 is a meiosis-specific cell cortex protein.** (A) Microscopic analysis of Mcp5 localization during meiosis. The *gfp-mcp5*[+] strain (ST329) was induced to enter meiosis by nitrogen starvation. For live observations, we added 0.5 μg/ml Hoechst 33342 to 200 μl of the cells and an aliquot was observed under a fluorescence microscope. After 6 h of incubation, the cells were subjected to microscopic observation. GFP-Mcp5 is green, CFP-Sad1 is red, and Hoechst 33342 staining is blue. (B) Typical image of fixed ST318. The microtubules are shown in red. Arrowheads indicate cortical Mcp5 dots adjacent to elongating microtubules. (C) Dhc1 colocalizes with Mcp5 at the cell cortex during horsetail phase. A drawing of the merged image is shown in the lower panels. ST359 was used for this observation. Typical images are shown. CFP-Mcp5 is in red, Dhc1-GFP is in green, and Hoechst 33342 staining is in blue. (D) Effect of overproducing Mcp5-GFP in mitotic cells. Mcp5-GFP was overproduced by transformation with the Mcp5-GFP expression vector *mcp5*[+]/pRGT1 in WT cells (CRL266). Bars, 10 μm.

"not sliding," depending on whether the microtubules curved or did not curve along the cell cortex, respectively. This analysis revealed that ∼50% of WT cells (Fig. 3, A [top] and B [left]) but only 12.8% of *mcp5Δ* cells (Fig. 3, A [bottom] and B [right]) exhibited sliding microtubules. This indicates that *mcp5Δ* cells are defective in the cortical sliding of their microtubules. It is known that Mcp6/Hrs1 plays an important role in organizing astral microtubule arrays at the SPB during the horsetail phase (Saito et al., 2005; Tanaka et al., 2005). However, *mcp5Δ* cells show normal localization of Mcp6/Hrs1 (unpublished data). Thus, it appears that although Mcp5 is not required for the proper formation of astral microtubules, it is needed for the proper sliding of the microtubules along the cell cortex.

Mcp5 is needed to anchor dyenin at the cell cortex during the horsetail phase
For Dhc1 to generate pulling force on the microtubule tip and so pull the SPB to the cortex, it must be fixed at the cell cortex. Dynein has both microtubule-binding and minus end–directed motor activity, and Yamamoto et al. (2001) proposed that a dynein anchor is required for dynein to accomplish these functions. To assess the role Mcp5 may play in this process, we investigated the localization of Dhc1-GFP during the horsetail phase in live observations (Fig. 3 C). In WT cells, the Dhc1-GFP dot was observed at the SPB and cell cortex along with the microtubules (Fig. 3, C [top] and D [left]; and Video 9, available at http://www.jcb.org/cgi/content/full/jcb.200512129/DC1). In contrast, most *mcp5Δ* cells did not exhibit an intense Dhc1-GFP dot at the cell cortex (Fig. 3, C [bottom] and D [right]; and Video 10). When we counted the number of cortical Dhc1-GFP dots, we found that 81% of WT but only 14% of *mcp5Δ* cells harbored these dots (Fig. 3 D, colored bars). Moreover, these

dots localized more frequently at the leading edge (57%) than on the tail side (24%) in WT cells, whereas the *mcp5Δ* cells showed a reversed trend (3 vs. 11%). These results suggest that horsetail movement is linked to the accumulation of cortical Dhc1-GFP dots and indicate that Mcp5 is required for anchoring dynein at the cell cortex, thus allowing the proper U-turn movement of the nucleus.

The PH domain is required for the cortical localization of Mcp5
To determine the function of the PH domain of Mcp5, we constructed the PH domain deletion mutant Mcp5 (PHΔ). When we overproduced the Mcp5 (PHΔ)-GFP fusion protein in *h*[90] WT cells (CRL266) using high-copy plasmid pREP1 driven by its *nmt1* promoter (Okuzaki et al., 2003), the cortical localization of Mcp5 was lost (Fig. 4 A). These results indicate that the PH domain is required for the cortical localization of Mcp5. Interestingly, most of the Mcp5 (PHΔ)-GFP signals were detected in the nucleus, and only a small amount of signal was observed along the microtubule (like Dhc1; Fig. 3 C) during both karyogamy and the horsetail phase (Fig. 4 A). It is possible that the PH-deleted Mcp5 mutant is transported to the nucleus through its nuclear localization signal (NLS). Furthermore, the Dhc1-like linear localization of Mcp5 (PHΔ) could signify that Mcp5 (PHΔ) is transported to the microtubules as a cargo protein of dynein.

Coiled-coil motifs are required for nuclear movement
To determine the role of the coiled-coil motif of Mcp5 plays, we prepared a mutant strain that expresses Mcp5 protein lacking two coiled-coil motifs, namely, Mcp5 (C-CΔ). When we overproduced the Mcp5 (C-CΔ)–GFP fusion protein in *h*[90] WT cells
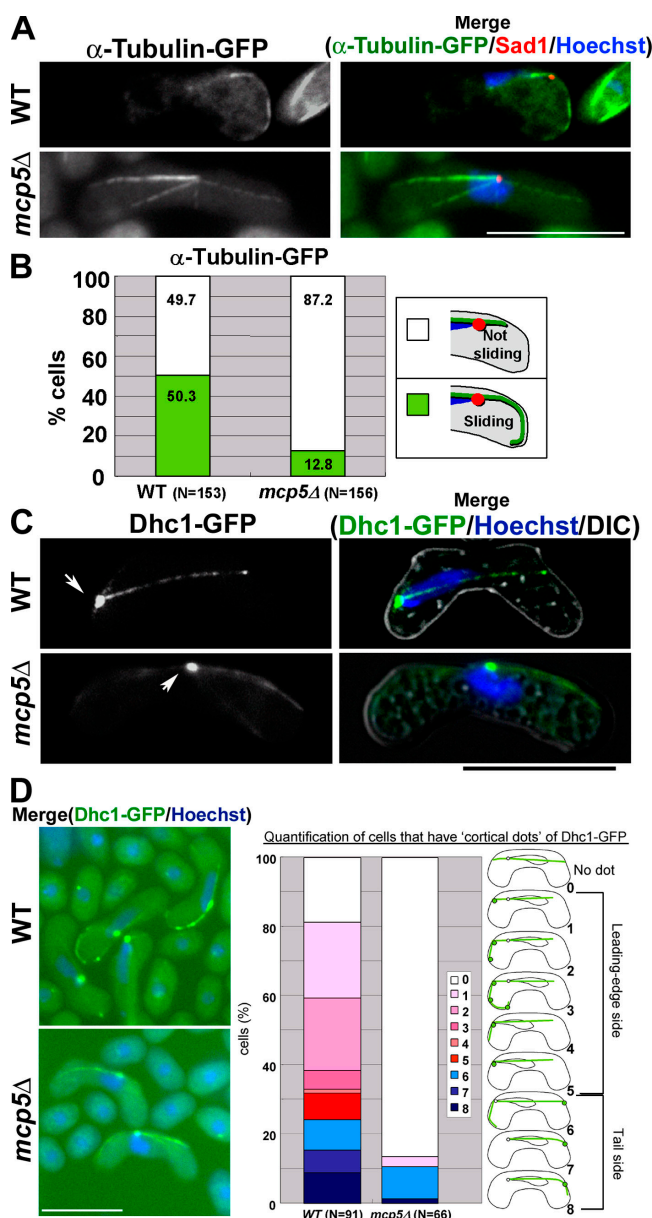
Figure 3. The cortical sliding of microtubules is abnormal in *mcp5Δ* cells. (A) Cells expressing α-tubulin–GFP (WT, YY105; *mcp5Δ*, ST218) were induced to enter meiosis by nitrogen starvation. After 6 h, the cells were fixed by glutaraldehyde and observed by microscopy. Typical images are shown. Green is α-tubulin–GFP, red is CFP-Sad1, blue is the Hoechst 33342–stained nucleus. Bar, 10 μm. (B) The frequency of cortically sliding microtubules. The green and white bars indicate the population of cells that harbor putatively sliding or not-sliding microtubules, respectively, as judged by the existence of curved or uncurved microtubules at the cell cortex. (C) Cell cortex localization of dynein is reduced in *mcp5Δ* cells. The *h⁹⁰* strains that express Dhc1-GFP (WT, CRL1526; *mcp5Δ*, ST254) were observed as living cells. The arrows indicate the localization of Dhc1 at the SPB. Green indicated Dhc1-GFP, and blue indicates Hoechst 33342. Bar, 10 μm. See Videos 9 and 10, available at http://www.jcb.org/cgi/content/full/jcb.200512129/DC1. (D) Quantitative analysis of cells bearing a cortical Dhc1-GFP dot. (left) Typical merged images. (right) Bar graphs showing the frequency of the cell types classified in the right panels. The leading-edge side signifies the cell edge toward which the SPB moves, whereas while the tail side signifies the opposite side.

(CRL266), it localized at the cell cortex (Fig. 4 B). These results indicate that the coiled-coil domain is not required for the cortical localization of Mcp5. We next observed the phenotypes of

the *mcp5 (c-cΔ)* strain during meiosis and found that it showed aberrant nuclear oscillation (Fig. 4 E), reducing the recombination rate (Fig. S2 C) and the abnormal spore formation (not depicted). These results indicate that the coiled-coil domain of Mcp5 plays a pivotal role in its full function and suggest that an unidentified partner that associates via the coiled-coil domain is involved in regulating nuclear movement.

Mcp5 anchors dynein and generates pulling force

Mcp5 localizes at the cell cortex via its PH domain (Fig. 4 A) and colocalizes with dynein (Dhc1) or tubulin-like Num1 of *S. cerevisiae* (Farkasovsky and Küntzel, 2001). Given that Num1 forms a transient complex in vivo with dynein and tubulin (Farkasovsky and Küntzel, 2001), it may be that Mcp5 also associates transiently with dynein and tubulin in vivo.

Fig. 5 illustrates our working hypothesis about the role Mcp5 plays in anchoring dynein and thereby generating pulling force. When the SPB (Fig. 5, gray circle) and the horsetail nucleus reaches at one end of the cell cortex, the microtubules carrying the SPB and nucleus extend toward the opposite end (Fig. 5 A). Pairing of homologous chromosomes may occur inefficiently in the round nucleus at the cell end. When the dynein complex (Fig. 5 A, green triangle) on the microtubules is trapped and anchored by Mcp5 (red circle), the minus-end motor activity may be stimulated (Fig. 5 B). Thus, the dynein starts to pull microtubules by its minus-end motor activity, which causes the cortical sliding of the microtubules. Then, the nucleus turns around and is pulled back toward the opposite cell end. Homologous chromosome pairing may be achieved widely in the elongated nucleus, which may induce the recombination of the homologous chromosomes. When the SPB arrives at the cell cortex where the dynein is anchored by Mcp5, the pulling force is gradually weakened and the microtubules behind the horsetail nucleus will extend to the opposite cell end, returning to stage A (Fig. 5 C). These stages are repeated several times during 2–3 h of prophase I. The magnified view of the cortical site on stage B is shown in Fig. 5 D. Like Num1 (Yu et al., 2004), Mcp5 is localized at the cell cortex, probably through its PH domain–mediated interaction with phosphatidylinositol (4,5) bisphosphate. Mcp5 on the membrane helps the cortical sliding of microtubules through anchoring the dynein–dynactin complex.

In conclusion, the homologous proteins Mcp5 and Num1 play similar roles in dynein-dependent nuclear migration (for review see Bloom, 2001; Yamamoto and Hiraoka, 2003), even though they are used in different cellular events, namely, Mcp5 in meiosis during prophase I and Num1 in mitosis during the budding (cell division) phase (Heil-Chapdelaine et al., 2000).

Materials and methods

Yeast strains, media, and molecular biology
The *S. pombe* strains used in this study are listed in Table S1 (available at http://www.jcb.org/cgi/content/full/jcb.200512129/DC1). The complete media YPD or YE, the synthetic Edinburgh minimal medium 2 (EMM2), and the sporulation medium molt extract or EMM2-nitrogen (EMM2-N; 1% glucose) were used. We used high-copy plasmid pREP1 driven by its *nmt1* promoter for overproduction experiments (Okuzaki et al., 2003).
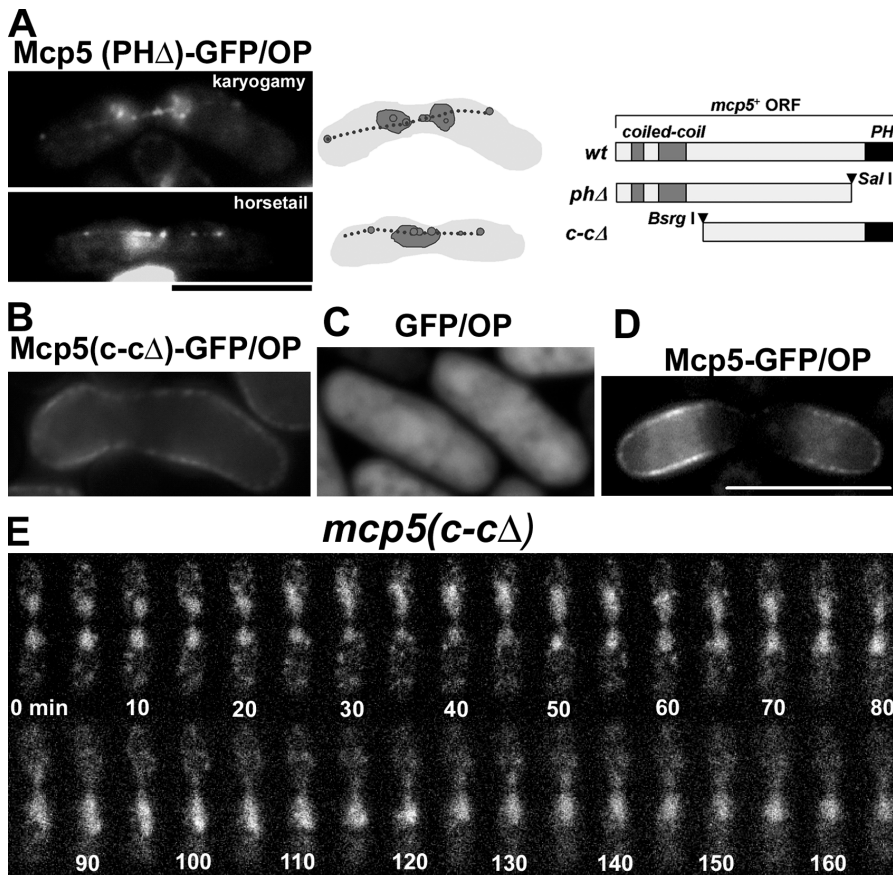
A
Mcp5 (PHΔ)-GFP/OP

karyogamy

horsetail

mcp5⁺ ORF

coiled-coil

PH

wt

phΔ

SalI

c-cΔ

BsrgI

B
Mcp5(c-cΔ)-GFP/OP

C GFP/OP

D Mcp5-GFP/OP

E *mcp5(c-cΔ)*

0 min 10 20 30 40 50 60 70 80

90 100 110 120 130 140 150 160

Figure 4. **The PH domain is required for the cortical localization of Mcp5.** (A) Constructs of deletion mutants are shown on the right. Subcellular localization of overproduced Mcp5 (PHΔ)-GFP. Typical images (karyogamy and horsetail phase) observed under a fluorescent microscope are shown. The Mcp5 (PHΔ)-GFP signals are interpreted in the right schemes. Bar, 10 μm. (B–D) Subcellular localization of overproduced Mcp5 (C-CΔ)-GFP (B), overproduced GFP (C, control), and overproduced Mcp5-GFP (D). These expression constructs were transformed into WT cells (CRL266). Bar, 10 μm. (E) Time-lapse observation of nuclear movement during prophase I in *mcp5 (c-cΔ)* mutant. Bar, 5 μm.

Time-lapse observations

For time-lapse observations, cells expressing GFP-tagged Polα (CRL026-1, ST205, and ST349) or lacI-NLS-GFP and the lacO repeat integrated at the *lys1* locus (AY174-7B and ST240) or *cut3* locus (NP43-20 and ST268) were cultured in 10 ml EMM2 + supplements until they reached midlog phase at 28°C. They were then induced to enter meiosis by incubation in EMM2-N at 28°C. After 5 h of nitrogen starvation, the cells were put on a glass-bottomed dish whose surface was coated with 0.2% concanavalin A, and images under a fluorescence microscope (IX71; Olympus) were recorded every 2.5 min (1 s of exposure time) after the initiation of karyogamy. For observation of lacI-GFP dots, images were taken with a 0.3-s exposure at 5-min intervals with 10 optical sections made at 0.5-μm intervals for each time point. Projected images obtained with MetaMorph software (Universal Imaging Corp.) were analyzed.

Construction of strains harboring integrated *GFP-mcp5⁺* and *mcp5⁺-FLAG* genes

For NH₂-terminal tagging to generate GFP-tagged *mcp5⁺*, we synthesized the following six oligonucleotides and used them as primers: MCP5-5F, 5′-AAAACTGCAGCTACGGCGGATTAAGGGTAG-3′; MCP5-5R, 5′-GGG-TTTCATATGGAAGGATCAGTATATGTTTTG -3′; Xho-mcp5N, 5′-CCGCTCGAGCGGATGGAGAAAAAACAAGATAACG-3′; Sma-mcp5C, 5′-TCCCCCGGGTTAAATGCCGGGCTTAGTATC-3′; MCP5-3F, 5′-TCCCCCGGGGGCATGTTTCAGTCATTGC-3′; and MCP5-3R, 5′-CTCG-AGGAGCTCCTTACAAAATAAAAATGCTG-3′. The underlined sequences denote the artificially introduced restriction enzyme sites for PstI, NdeI, XhoI, SmaI, SmaI, and SacI, respectively. These PCR products were inserted into the pRGT1 vector via the PstI–NdeI, XhoI–SmaI, and SmaI–SacI sites, respectively. This plasmid construct was digested with PstI and SacI, and the resulting construct was introduced into the *mcp5⁺::ura4⁺* strain ST256. After growth on EMM2 + 5-fluoroorotic acid plates, the ura transformants were screened by PCR analysis to identify the (*mcp5⁺::ura4⁺*)::(*GFP-mcp5⁺*) replacement.

For COOH-terminal tagging to generate FLAG-tagged *mcp5⁺*, we followed the previously described method (Saito et al., 2004). Thus, we performed PCR using the WT (TP4-5A) genome as a template and obtained a DNA fragment carrying the ORF and the 3′ downstream region

of the *mcp5⁺* gene. For this purpose, we synthesized the following two oligonucleotides and used them as primers: MCP5N, 5′-CGGCGCGC-CGCATATGGAGAAAAAACAAGATAA-3′, and MCP5C, 5′-GTACTCG-AGGCGGCCGCGGAATGCCGGGCTTAGTATCAA-3′. The underlined sequences denote the artificially introduced restriction enzyme sites for NdeI and NotI, respectively. To obtain the 3′ downstream region, we used the primers described in the previous paragraph that produce the SmaI–SacI fragment. These PCR products were inserted into the pTT (FLAG)-Lys3 vector (Saito et al., 2005), which is designed to allow one-step integration. This plasmid construct was digested with NsiI. The resulting construct was introduced into HM105 (*h⁻ lys3*). We then screened the Lys+ transformants and confirmed the precise integration of the constructs by PCR.

Fluorescent microscopic observation and immunofluorescence

Fluorescent microscopic observations were performed as described previously (Saito et al., 2005). Cells from a single colony were cultured in 10 ml EMM2 with supplements until they reached midlog phase at 28°C. The cells were collected by centrifugation, washed three times with 1 ml EMM2-N, and induced to enter meiosis by incubation in EMM2-N at 28°C for 6 h.

For immunofluorescence experiments, meiotic cells were fixed after the procedure using methanol or glutaraldehyde. For methanol fixation, cells were collected by aspiration through a glass filter that traps cells. The cells were immediately immersed into methanol at –80°C and left overnight to fix the cells. The cells were then washed off the glass filter by distilled water and collected by centrifugation, and the pellet was washed three times with PBS. For glutaraldehyde fixation, 10 ml of cultured cells were incubated in ~3% paraformaldehyde and 0.25% glutaraldehyde for 1 h.

In indirect immunofluorescence microscopy, microtubules were stained with the anti–α-tubulin antibody TAT1 (after methanol fixation; a gift from K. Gull, University of Manchester, Manchester, UK) and the SPB was stained with the anti-Sad1 antibody (after glutaraldehyde fixation; a gift from O. Niwa, Kazusa DNA Research Institute, Kisarazu, Japan). Subsequently, we added an Alexa 594–conjugated goat anti–mouse antibody (Invitrogen) for TAT1 or an Alexa 594–conjugated goat anti–rabbit antibody (Invitrogen) for the anti-Sad1 antibody, respectively. In both cases, the samples were then stained with 0.2 mg/ml Hoechst 33342 in PBS for 1 min and mounted with antifade mounting medium containing
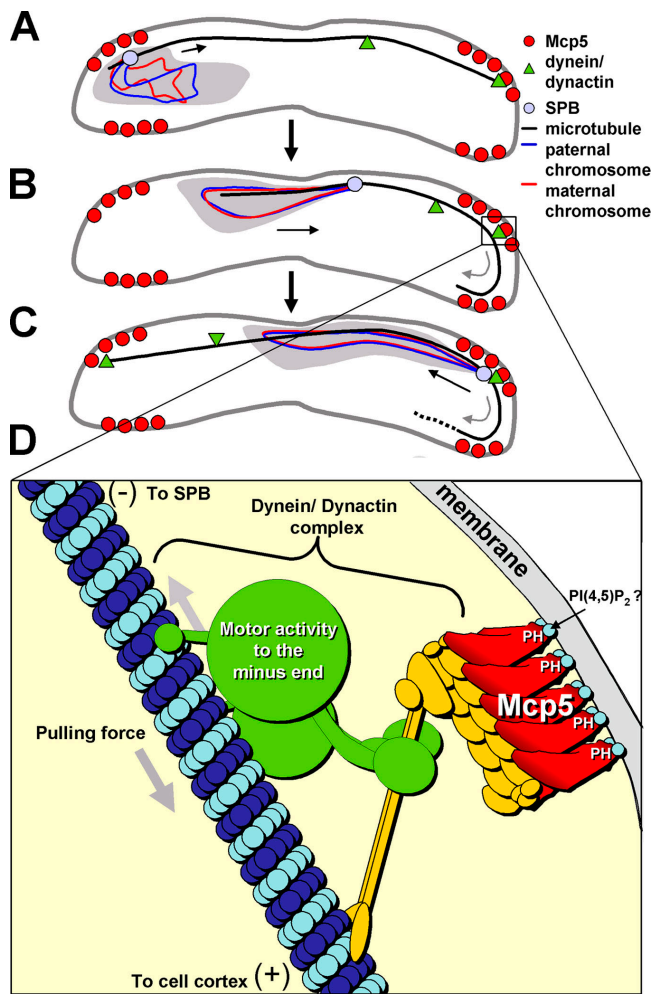
Figure 5. A possible model to explain how Mcp5 controls generation of pulling force by anchoring dynein. During the horsetail phase of fission yeast, astral microtubules may elongate and reach to the cell cortex (A), where they may slide (B) to pull the nucleus (C). When Mcp5 anchors the dynein at the cortex, microtubules may be pulled up because of the minus-end motor activity of dynein (D). Thus, nuclear oscillation may be induced by repetition of this process. See text for details.

p-phenylenediamine. Fluorescence images of these cells were observed using a fluorescence microscope (BX51; Olympus) with a charge-coupled device camera (CoolSNAP; Roper Scientific). Immunofluorescence images were acquired using Photoshop 7.0 (Adobe).

Online supplemental material
Fig. S1 shows that Mcp5 is a meiosis-specific coiled-coil protein that belongs to Num1 family proteins found specifically among fungi. Fig. S2 shows characterization of *mcp5Δ* cells. Video 1 shows a wild-type cell expressing GFP-labeled DNA polymerase α during zygotic meiosis. Video 2 shows an *mcp5Δ* cell expressing GFP-labeled DNA polymerase α during zygotic meiosis. Video 3 shows a wild-type cell expressing GFP-labeled DNA polymerase α during azygotic meiosis. Video 4 shows an *mcp5Δ* cell expressing GFP-labeled DNA polymerase α during azygotic meiosis. Video 5 shows a wild-type cell whose *lys1* loci are labeled by GFP-LacI-NLS fusion protein. Video 6 shows an *mcp5Δ* cell whose *lys1* loci are labeled by GFP-LacI-NLS fusion protein. Video 7 shows a wild-type cell whose *cut3* loci are labeled by GFP-LacI-NLS fusion protein. Video 8 shows an *mcp5Δ* cell whose *cut3* loci are labeled by GFP-LacI-NLS fusion protein. Video 9 shows a wild-type cell expressing GFP-labeled Dhc1 during horsetail phase. Video 10 shows an *mcp5Δ* cell expressing GFP-labeled Dhc1 during horsetail phase. Table S1 shows a list of strains used in this study. Online supplemental material is available at http://www.jcb.org/cgi/content/full/jcb.200512129/DC1.

References

Bloom, K. 2001. Nuclear migration: cortical anchors for cytoplasmic dynein. *Curr. Biol.* 11:R326–R329.

Chikashige, Y., D.Q. Ding, H. Funabiki, T. Haraguchi, S. Mashiko, M. Yanagida, and Y. Hiraoka. 1994. Telomere-led premeiotic chromosome movement in fission yeast. *Science.* 264:270–273.

Ding, D.Q., Y. Chikashige, T. Haraguchi, and Y. Hiraoka. 1998. Oscillatory nuclear movement in fission yeast meiotic prophase is driven by astral microtubules, as revealed by continuous observation of chromosomes and microtubules in living cells. *J. Cell Sci.* 111:701–712.

Ding, D.Q., A. Yamamoto, T. Haraguchi, and Y. Hiraoka. 2004. Dynamics of homologous chromosome pairing during meiotic prophase in fission yeast. *Dev. Cell.* 6:329–341.

Farkasovsky, M., and H. Küntzel. 2001. Cortical Num1p interacts with the dynein intermediate chain Pac11p and cytoplasmic microtubules in budding yeast. *J. Cell Biol.* 152:251–262.

Fischer, R., and W.E. Timberlake. 1995. *Aspergillus nidulans apsA* (anucleate primary sterigmata) encodes a coiled-coil protein required for nuclear positioning and completion of asexual development. *J. Cell Biol.* 128:485–498.

Graïa, F., V. Berteaux-Lecellier, D. Zickler, and M. Picard. 2000. *ami1*, an orthologue of the *Aspergillus nidulans apsA* gene, is involved in nuclear migration events throughout the life cycle of *Podospora anserina. Genetics.* 155:633–646.

Harper, L., I. Golubovskaya, and W.Z. Cande. 2004. A bouquet of chromosomes. *J. Cell Sci.* 117:4025–4032.

Heil-Chapdelaine, R.A., J.R. Oberle, and J.A. Cooper. 2000. The cortical protein Num1p is essential for dynein-dependent interactions of microtubules with the cortex. *J. Cell Biol.* 151:1337–1344.

Hiraoka, Y. 1998. Meiotic telomeres: a matchmaker for homologous chromosomes. *Genes Cells.* 3:405–413.

Kohli, J. 1994. Meiosis: telomeres lead chromosome movement. *Curr. Biol.* 4:724–727.

Kormanec, J., I. Schaaff-Gerstenschlager, F.K. Zimmermann, D. Perecko, and H. Kuntzel. 1991. Nuclear migration in *Saccharomyces cerevisiae* is controlled by the highly repetitive 313 kDa NUM1 protein. *Mol. Gen. Genet.* 230:277–287.

Martin-Castellanos, C., M. Blanco, A.E. Rozalen, L. Perez-Hidalgo, A.I. Garcia, F. Conde, J. Mata, C. Ellermeier, L. Davis, P. San-Segundo, et al. 2005. A large-scale screen in *S. pombe* identifies seven novel genes required for critical meiotic events. *Curr. Biol.* 15:2056–2062.

Miki, F., K. Okazaki, M. Shimanuki, A. Yamamoto, Y. Hiraoka, and O. Niwa. 2002. The 14-kDa dynein light chain-family protein Dlc1 is required for regular oscillatory nuclear movement and efficient recombination during meiotic prophase in fission yeast. *Mol. Biol. Cell.* 13:930–946.

Niccoli, T., A. Yamashita, P. Nurse, and M. Yamamoto. 2004. The p150-Glued Ssm4p regulates microtubular dynamics and nuclear movement in fission yeast. *J. Cell Sci.* 117:5543–5556.

Niwa, O., M. Shimanuki, and F. Miki. 2000. Telomere-led bouquet formation facilitates homologous chromosome pairing and restricts ectopic interaction in fission yeast meiosis. *EMBO J.* 19:3831–3840.

Okuzaki, D., W. Satake, A. Hirata, and H. Nojima. 2003. Fission yeast *meu14+* is required for proper nuclear division and accurate forespore membrane formation during meiosis II. *J. Cell Sci.* 116:2721–2735.

Saito, T.T., T. Tougan, T. Kasama, D. Okuzaki, and H. Nojima. 2004. Mcp7, a meiosis-specific coiled-coil protein of fission yeast, associates with Meu13 and is required for meiotic recombination. *Nucleic Acids Res.* 32:3325–3339.

Saito, T.T., T. Tougan, D. Okuzaki, T. Kasama, and H. Nojima. 2005. Mcp6, a meiosis-specific coiled-coil protein of *Schizosaccharomyces pombe*, localizes to the spindle pole body and is required for horsetail movement and recombination. *J. Cell Sci.* 118:447–459.

Shimanuki, M., F. Miki, D.Q. Ding, Y. Chikashige, Y. Hiraoka, T. Horio, and O. Niwa. 1997. A novel fission yeast gene, *kms1*[+], is required for the formation of meiotic prophase-specific nuclear architecture. *Mol. Gen. Genet.* 254:238–249.

Tanaka, K., T. Kohda, A. Yamashita, N. Nonaka, and M. Yamamoto. 2005. Hrs1p/Mcp6p on the meiotic SPB organizes astral microtubule arrays for oscillatory nuclear movement. *Curr. Biol.* 15:1479–1486.

Yamamoto, A., and Y. Hiraoka. 2003. Cytoplasmic dynein in fungi: insights from nuclear migration. *J. Cell Sci.* 116:4501–4512.

Yamamoto, A., R.R. West, J.R. McIntosh, and Y. Hiraoka. 1999. A cytoplasmic dynein heavy chain is required for oscillatory nuclear movement of meiotic prophase and efficient meiotic recombination in fission yeast. *J. Cell Biol.* 145:1233–1249.

Yamamoto, A., C. Tsutsumi, H. Kojima, K. Oiwa, and Y. Hiraoka. 2001. Dynamic behavior of microtubules during dynein-dependent nuclear migrations of meiotic prophase in fission yeast. *Mol. Biol. Cell.* 12:3933–3946.

Yamashita, A., Y. Watanabe, and M. Yamamoto. 1997. Microtubule-associated coiled-coil protein Ssm4 is involved in the meiotic development in fission yeast. *Genes Cells.* 2:155–166.

Yu, J.W., J.M. Mendrola, A. Audhya, S. Singh, D. Keleti, D.B. DeWald, D. Murray, S.D. Emr, and M.A. Lemmon. 2004. Genome-wide analysis of membrane targeting by *S. cerevisiae* pleckstrin homology domains. *Mol. Cell.* 13:677–688.